The IR spectrum of supercritical water: Combined molecular dynamics/quantum mechanics strategy and force field for cluster sampling

Patrice Bordat, Didier Bégué, Ross Brown, Alain Marbeuf, Henri Cardy, Isabelle Baraille

The IR Spectrum of Supercritical Water: Combined Molecular Dynamics/Quantum Mechanics Strategy and Force Field for Cluster Sampling

P. Bordat,*[a] D. Bégué,*[a] R. Brown,[a] A. Marbeuf,[b] H. Cardy,[a] and I. Baraille[a]

Supercritical water was analyzed recently as a gas of small clusters of waters linked to each other by intermolecular hydrogen-bonds, but unexpected 'linear" conformations of clusters are required to reproduce the infra-red (IR) spectra of the supercritical state. Aiming at a better understanding of clusters in supercritical water, this work presents a strategy combining classical molecular dynamics to explore the potential energy landscape of water clusters with quantum mechanical calculation of their IR spectra. For this purpose, we have developed an accurate and flexible force field of water based on the TIP5P 5-site model. Water dimers and trimers obtained with this improved force field compare well with the quantum mechanically optimized clusters. Exploration by simulated annealing of the potential energy surface of the classical force field reveals a new trimer conformation whose IR response determined from quantum calculations could play a role in the IR spectra of supercritical water.

Introduction

Water uniquely combines both highly anomalous properties compared with many solvents, and paramount importance in practical and industrial chemistry and in biology. The supercritical state is the most recent subject of the longstanding interest in the physical and chemical properties of water.[1–3] Among the unusual properties of supercritical water are: dielectric constant, viscosity, and solvating ability.[4] Applications of these properties include oxidation of industrial waste,[5] some chemical reactions and synthesis without the need for catalysis,[6] and control of reaction kinetics.[7]

Naturally, one would like to understand how these properties are related to the difference in molecular and intermolecular structure and dynamics of supercritical and ordinary water. The structure of supercritical water has been investigated using X-rays,[8,9] neutron scattering experiments,[10] and more recently by inelastic X-ray scattering.[11] Proton NMR experiments have been performed to measure the self-diffusion of water[12] and the degree of hydrogen bonding under supercritical conditions.[13,14] Raman scattering,[15,16] infrared absorption[7,17–21] as well as time resolved spectroscopy[22] have shown qualitatively how the degree of hydrogen bonding in pure water changes with temperature and pressure. It was concluded from all these experiments that hydrogen bonds persist in supercritical water and the degree of hydrogen bonding was found to depend strongly upon the pressure and temperature. The current picture of supercritical water is a state akin to a gas of small clusters of hydrogen bonded water molecules (H bonds).

The sensitivity of the intramolecular stretch and bend vibrational frequencies of water to hydrogen bonds with neighboring molecules makes near- and mid-infra-red (IR) spectroscopies appealing tools for investigating these clusters, particularly when interpreted with the help of molecular simulation. On the one hand, molecular dynamics and Monte Carlo simulations provide information on the nature and dynamics of the water clusters.[7,23–26] On the other, quantum chemistry may identify particularly stable small clusters (in fact mostly dimers and trimers) and the specific signature of the perturbing influence of H bonds on the intramolecular IR frequencies (and intensities) of each type of the cluster. Not surprisingly in this approach, cyclic H-bonded clusters are found to be more stable than linear structures of the same size.

In earlier work, we found the proportions of these small clusters in supercritical water by fitting a weighted sum of the predicted IR bands to the experimental spectra, yielding good agreement with the experimental fundamental, combination and overtone bands, over a range of pressures at 380°C.[27,28] However, we found an anomalously high proportion of linear rather than cyclic clusters, compared with the ratios deduced

[a] *P. Bordat, D. Bégué, R. Brown, H. Cardy, I. Baraille*
Institut Pluridisciplinaire de recherche sur l'Environnement et les Matériaux (IPREM), UMR 5254, CNRS Equipe de Chimie Physique, Université de Pau et des Pays de l'Adour, 2 avenue du Président Angot, 64053 Pau Cedex 9, France
E mail: patrice.bordat@univ pau.fr (or)
didier.begue@univ pau.fr

[b] *A. Marbeuf*
Laboratoire Onde et Matière d'Aquitaine, Université Bordeaux 1, UMR 5798, 351 cours de la Libération, 33405 Talence, Cedex, France

Contract grant sponsor: Centre Informatique National de l'Enseignement Supérieur (CINES).
Contract grant sponsor: Conseil Regional d'Aquitaine.
Contract grant sponsor: French Ministry of Research and Technology.

from thermal equilibrium and the potential energies of the optimized model clusters. Bearing in mind the temperatures and pressures involved (critical point 374.15°C, 217.7 bar), we thus ask two questions:

a. Are the linear clusters present in supercritical water and what is the physical mechanism responsible for their appearance despite unfavorable thermal population factors?

b. Are the IR bands predicted for the energy-minimized structures the only relevant data to describe the spectrum of supercritical water?

Both questions imply broad sampling of the total potential energy surface of water, under supercritical thermodynamic conditions, which today still means long (nanoseconds) classical molecular dynamics or Monte Carlo simulation of large models (hundreds of molecules), accommodating the formation, collision, and decay of clusters. But only sophisticated quantum chemistry can predict the positions and intensities of the near- and mid-IR bands with sufficient accuracy to fully draw out all the information in the remarkably structured experimental spectra. However, this quantum mechanical (QM) approach requires solution of the vibrational Schrödinger equation on a potential energy surface determined by expensive, high level electronic structure computations. Clearly, a compromise is necessary. Our opinion is that there are two main points: the relevance of energy minimized structures to supercritical conditions and sufficient sampling of the potential energy surface. We therefore propose a five-pronged strategy:

1. Screen possible candidate clusters of water molecules by simulated annealing in classical molecular dynamics simulations.

2. Optimize these candidates in accurate QM calculations. Estimate their IR bands by solution of the vibrational Schrödinger equation on the QM energy surface.

3. Search a classical simulation of supercritical water on the fly, for the clusters identified in step (1) (and others that may occur).

4. Use the spectra from (2) and the statistical weights from (3) to predict the experimental spectrum.

5. Solve the vibrational Schrödinger equation and compute the IR spectrum using the classical potential energy surface in lieu of the QM one. When compare with the spectrum obtained from the classical simulation of supercritical water by Fourier transformation of the fluctuations of the dipole moment.

Points (1)–(4) are intended to improve our current method of computing the spectrum, hence to answer question (a). Point (5) should help answer question (b): Rather than comparing the spectrum predicted from the QM energy minima with the experimental spectrum, for which the "electronic energy surface" is unknown and surely different, we suggest comparing the QM spectrum with an "experiment" (molecular dynamics) with a known, simple potential energy surface. Because the molecular dynamics force field is carried over to the QM computation in step (5), any discrepancies between the classical spectra and those QM-derived from the optimized structures should highlight shortcomings of representing the "real" system (the molecular dynamics simulation) with only minimized structures. This article illustrates steps (1–2).

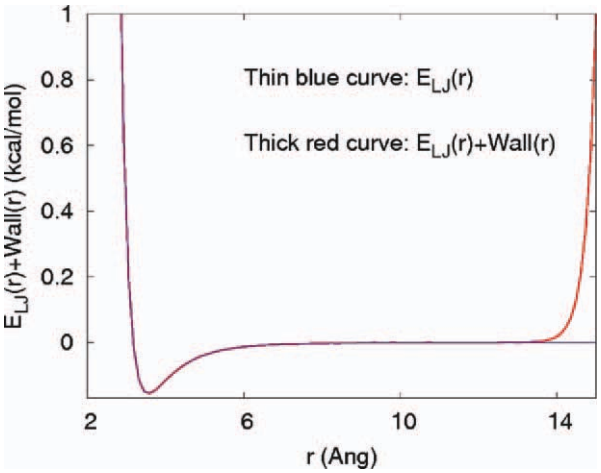

Figure 1. Standard intermolecular Lennard Jones potential energy term between oxygen atoms of water in blue, and the modified (red) with a restraining wall at $r = 15$ Å.

Before carrying out this program, one obviously would prefer the classical mechanical model of water to reproduce as far as possible the QM-determined clusters and their properties, while retaining compatibility with the experimentally known properties of supercritical water. In this work, we therefore develop intramolecular force-fields to describe the structure of the water molecule and its vibrational modes, in agreement with experimental data and *ab initio* calculations. These force-fields are combined in simulated annealing in molecular dynamics simulations, with an intermolecular force field in which the water molecule originally was represented as a rigid unit, TIP/5P. We thus find cluster conformers missed in our earlier search.

Computational Procedures

Simulated annealing

We used the molecular dynamics package DL POLY 2.20[29,30] for simulated annealing on the potential energy surface of the water dimer and trimer. Long simulations of isolated clusters (5×10^6 steps) were performed in the canonical ensemble, at a temperature of 450 K in a cubic box, side 40 Å. The cutoff radius for nonbonded interactions was 18.5 Å, and the time-step 0.5 fs. Electrostatic interactions were evaluated with the Ewald approximation. Every 5000 steps, we quenched the instantaneous structure to 1 K for 10^5 timesteps. 1000 minimizations were performed along the "hot" trajectory. The high temperature favors efficient exploration of the energy surface, but also favors evaporation of the cluster. We could effectively

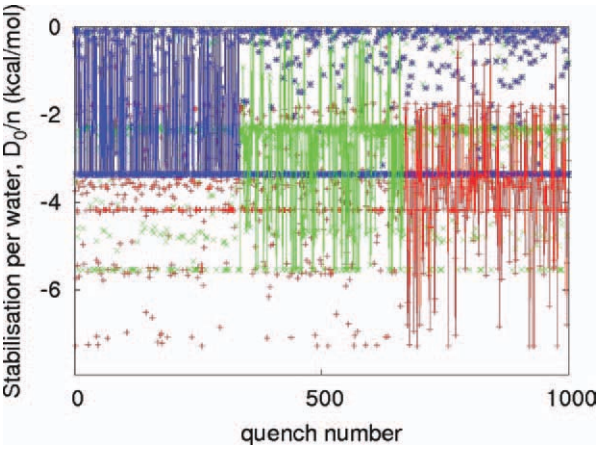

Figure 2. Configurational energy stabilization per molecule (relative to free molecules) $D_0/n = (E_{pot}((H_2O)_n) - nE_{pot}(H_2O))/n$ for 1000 structures quenched from 'hot' MD simulations of small water clusters, $n = 2$ 4,: dimer (blue, *), trimer (green, ×), and tetramer (red, +). Lines: Connected portions of each quench history highlight the absence of correlation between successive quenches.

counter this tendency by adding a restraining potential energy term between any pair of oxygen atoms, with the form $W(r) = A \exp(-\alpha(r - r_m))$, where $A = 1$ kcal/mol, $r_m = 15$ Å, and $\alpha = 4$ Å^{-1}, see Figure 1. The restraining potential does not affect the structures and energies of the minimized clusters.

Figure 2 shows that the structure reached in the quenches changes frequently along the hot trajectory. We believe that most if not all the minima have been found. Note that in this size range, the stabilization energy per molecule increases faster than the number of molecules, n, because of H-bonding in cyclic and partially cyclic clusters. We concentrate below on the dimer and trimer because it is already known that tetramer contributes little to the experimental IR spectrum of supercritical water.[27,28]

Development of a flexible classical model

We developed flexible models of water, starting from two well-known rigid body models of bulk water, by replacing the rigid body by a flexible molecule with intramolecular bond stretch and bend terms. Parameters were optimized with respect to the experimental anharmonic and harmonic vibrational frequencies of water (see Table 1).

The OH bond was represented by a Morse potential: $E_{OH}(r) = E_0\{[1 - \exp(-k(r - r_0)]\}^2$, where E_0 is the well depth, r_0 the equilibrium distance, and k determines the curvature. Coupling between the OH bonds is represented by a cross term: $E(r_{12},r_{13}) = k_c(r_{12} - r_0)(r_{13} - r_0)$, where is r_{12} and r_{13} are the distances between the oxygen atom (1) and the hydrogens (2,3). The HOH angle, θ, moves under the influence of the potential energy term $E(\theta) = \frac{1}{2}k_\theta(\theta - \theta_0)^2$, with reference value θ_0.

We used the theoretical position and depth of the OH potential well in the water molecule (CCSD(T)/aug-ccpVTZ) to determine $r_0 = 0.96$ Å, k and $\theta_0 = 104.5^\circ$. Experimental bend and stretch harmonic frequencies (Table 1) further restrict the choice of the force constants k and k_θ. Finally, the difference between the antisymmetric and symmetric stretch frequencies fixes k_c. After which E_0 and k must be slightly adjusted.

We thus first extended the SPC/E model of water, but quickly abandoned it, because it leads to a planar cyclic structure as the lowest trimer configuration, in contradiction to *ab initio* calculations,[27] in which half the hydrogens lie out of the plane of the oxygen atoms. The root of the problem is that in an H-bond, OH O, hydrogen interacts with a lone pair of the second oxygen. The overall tetrahedral arrangement of the hydrogens and the lone pairs around the oxygen then drives one of the hydrogens of the second molecule out of the plane of the cyclic trimer, the other pointing to the third oxygen atom (again through a lone pair). Several models of water allow for the lone pairs. We adapted our intramolecular interaction terms to the TIP5P model,[17] which originally specified a rigid molecule with the parameters: OH = 0.9572 Å, HOH = 104.52°, OL = 0.7 Å, where L is a negative point charge to represent a lone pair, with LOL = 109.47°.

Tables 2 and 3 provide the parameters of our flexible TIP5P model of water. Whereas in the original TIP5P model, the L sites are massless, DL POLY 2.20 requires all centers of force to have finite mass. In our extension of the model, LOL is therefore a rigid unit with atomic masses $m_O = 15.679$, $m_L = 0.16$, a compromise which keeps the moments of inertia of the modified 5 site model very close to those of the original. We tuned two sets of parameters, set I to reproduce the experimental harmonic vibrational frequencies to within 0.1 cm^{-1} and set II relative to the observed anharmonic frequencies.

Table 2. Parameters of the Lennard Jones interactions between oxygen atoms

σ (Å)	3.12
ε (kcal/mol)	0.155
q_O (e)	0.000
q_H (e)	+0.241
q_L (e)	0.241

Partial charges in the TIP5P model of water.

Table 1. Experimental observed (anharmonic) and harmonic vibrational frequencies of water.

	Observed frequency (cm^{-1})	Harmonic frequency (cm^{-1})
Modes	Refs. [31,32]	Our work
Bending	1594.75	1648.5
Symmetric stretching	3657.05	3832.2
Antisymmetric stretching	3755.8	3942.5

Table 3. Intramolecular force field parameters in this work.

	Set I	Set II
E_0 (kcal/mol)	116.609	106.135
k (Å^{-1})	2.2805	2.2805
r_0 (Å)	0.96	0.96
k_c (kcal/mol/Å^2)	16.66655	13.59655
$r_{12} = r_{13}$ (Å)	0.96	0.96
k_θ (kcal/mol/rad^2)	99.4433	93.1886
θ (°)	104.5	104.5

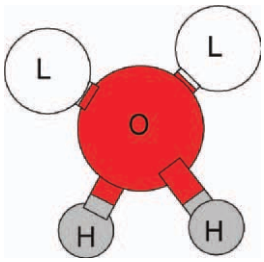

Figure 3. Modified flexible model of water derived from the TIP5P 5 site. LOL is a rigid unit. All other degrees of freedom are free. [Color figure can be viewed in the online issue, which is available at wileyonlinelibrary.com.]

Quantum mechanical calculations

The QM calculations closely follow the procedures of Tassaing et al.,[27,28] including both mechanical and electrical anharmonicity at a B1LYP/cc-pVTZ level of calculation. Briefly, the modeling of specific vibrations requires well-adapted mathematical approaches like the variational one. Despite the existence of efficient specific perturbational treatments, often sufficient to describe the fundamental modes, an extensive vibrational configuration space obtained in a variational development is essential to correctly describe resonant phenomena which arise when considering overtones and combinations bands.[27,33–35] In our case, the vibrational Schrödinger equation has been solved by our P MWVCI (Parallel Multi Windows Variational CI) variational procedure considering the rotational contribution to anharmonicity in the vibrational Hamiltonian implemented in the P Anhar v1.2 code.[35] Anharmonic activities are also computed with the use of a variational approach developed in the last version of the P Anhar code.[27]

In this work, four spectral regions were examined (in term of trimer nomenclature): HOH bend, ν_1–ν_3, [1570:1640] cm^{-1}, symmetrical and anti-symmetrical OH stretching, ν_4–ν_9, [3400:3800] cm^{-1}, the first bend-stretch combination band, [5250:5380] cm^{-1}, and the first stretch harmonic overtone ν_{OH}, [7150:7350] cm^{-1}. The width and density of states of these regions required over 10,000 vibrational configurations in each variational process to ensure convergence of all states in all regions to within 0.1 cm^{-1}.

Results

Classical screening of water trimer conformers

Figure 4 displays the dimer conformation and four trimer conformations identified in the simulated annealing procedure. We find both cyclic and linear structures. On the whole, the lowest energy structures are cyclic, and in each category, the higher the degree of regular donor–acceptor H-bond alternation, the lower the energy. Considering the number of quenches in the simulated annealing and the absence of correlation between successive quenches, we believe that we have found most of the minima of the molecular mechanics potential energy surface. This is step (1) of the strategy described above. When compared with the earlier, much more costly and hence less exhaustive search by quantum mechanics alone,[27,28] the present search threw up new minima, such as the "4d" trimer (cf. Fig. 4d). In step (2) below, we optimize the candidate structures quantum mechanically and compute their IR spectra.

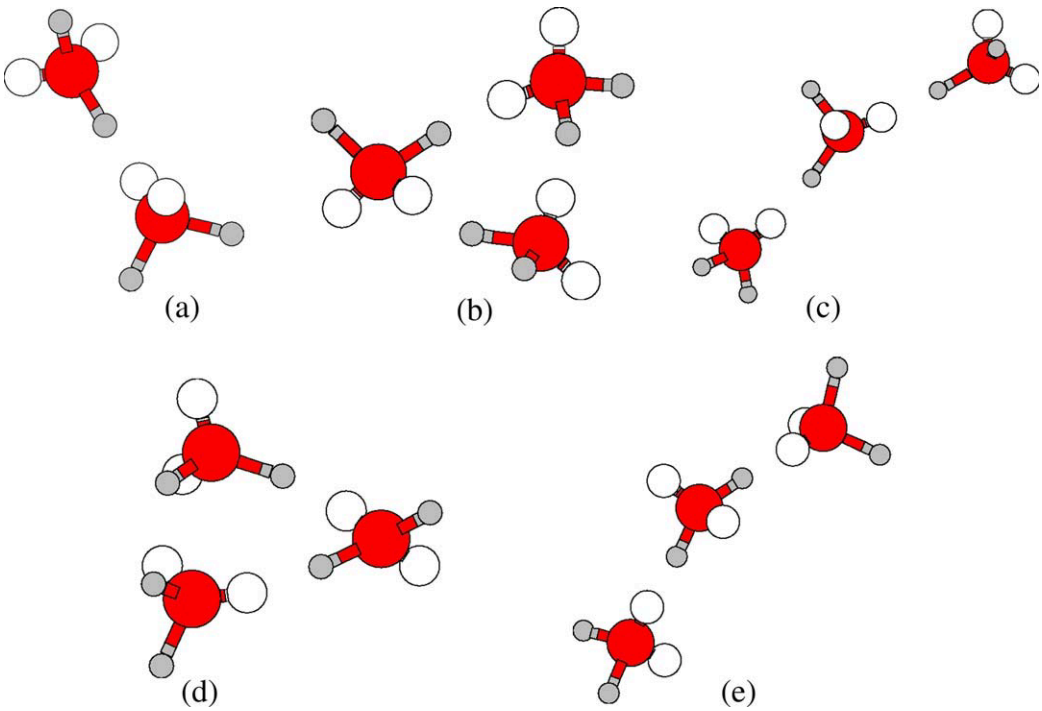

Figure 4. Dimer and trimer conformations obtained with the present flexible TIP5P model of water: a) Lowest dimer (D_0 = 6.73 kcal/mol); b) Lowest trimer (D_0 = 5.54 kcal/mol), with cyclic alternation of donor acceptor H bonds in the plane of the oxygens; c) The lowest linear trimer (D_0 = 4.59 kcal/mol), with regular alternation of donor acceptor bonds; d) A cyclic trimer with double acceptor H bonds on one molecule (D_0 = 4.10 kcal/mol); e) A higher linear trimer (D_0 = 3.85 kcal/mol), with a double donor molecule.

QM derived properties and spectra of the conformers

Reoptimization is important for obtaining accurate harmonic frequencies, which are well known to depend strongly on the geometry of the system. The structures quenched in molecular dynamics are close, but not identical to the corresponding QM minima (Table 4). The mean deviation of the QM vibronic frequencies between the as-quenched and the reoptimized system 4d is thus 40 cm^{-1}, precluding direct reliable comparison with the fine details of the experimental spectra. On the other hand, classical screening, which is much less expensive than QM computation, allows thorough exploration of the complete energy surface.

Table 4. Properties of water clusters optimized at both the B1LYP/cc pVTZ and molecular dynamics (italic) levels includes corrections for ZPE and BSSE.

		$(H_2O)_2$	$(H_2O)_3$			
Figure 4	H_2O	4a	4b	4c	4d	4e
D_0 (kcal/mol)		3.18	13.21	7.10	6.14	5.10
		6.73	*16.63*	*13.78*	*12.31*	*11.55*
		[3.6 ± 0.5][a] 3.53[b] 3.09[c] 5.18[d] 2.98[e]	12.71[b] 10.88[c] 15.90[d]			
$d_{O\ O}$ (Å)	0.96[f]	2.92	2.79(2)	2.83	3.36	2.97(2)
	0.96	*2.71*	*2.73*	*2.75*	*3.21*	*2.73*
	[0.9572][g,h]	[2.98][a] 2.90[c] 2.92[i]	[2.94 2.97][a] 2.91[b] 2.79[i] 2.81[i]			2.90[j]
δ_{HOH} (°)	104.6	104.8 105.5	105.6 105.7	105.6 105.7	105.1	105.4 106.2
	104.4	*103.1 103.3*	*102.6 102.7*	*103.1 103.5*	*103.3*	*103.5*
	[104.52][g,h]	105.0 105.4[b] 104.2[e]	105.8 106.2[b]			
δ_{OHO} (°)		173.1	151.0 152.7	154.6 156.7	165.4	174.8
		176.8	*158.7 160.0*	*160.2 160.6*	*166.4*	*177.0*
		[174 ± 20][k] 173.8[b] 171.7[c]	150.0 151.9[b] 148.6 151.3[c]			

Experimental data in brackets.
[a] ($v = 0$), Ref. [36]. [b] DFT PP gradient corrected density functional, Ref. [37]. [c] MP2/aug cc pVTZ, Ref. [38]. [d] ΔE (TTM3 F potential), Ref. [39]. [e] CCSD(T)/aug cc pVTZ (avtz), Ref. [40]. [f] $d_{O\ H}$ value for the monomer. [g] Ref. [41]. [h] $d_{O\ H}$ (Å). [i] MP2/6 311++G(3d,3p), Ref. [42]. [j] MD, Refs. [2,38]. [k] Ref. [43].

The vibrational frequencies of trimer 4d were determined exactly as in our earlier work.[27,28] Figure 5 compares the spectra of 4d with those of the lowest linear trimer 4c,[27] which is only 1.5 kcal/mol lower than 4d, and of the linear trimer 4e, which was thought to be the most frequent cluster appearing in supercritical conditions.[28] We observe from these data that:

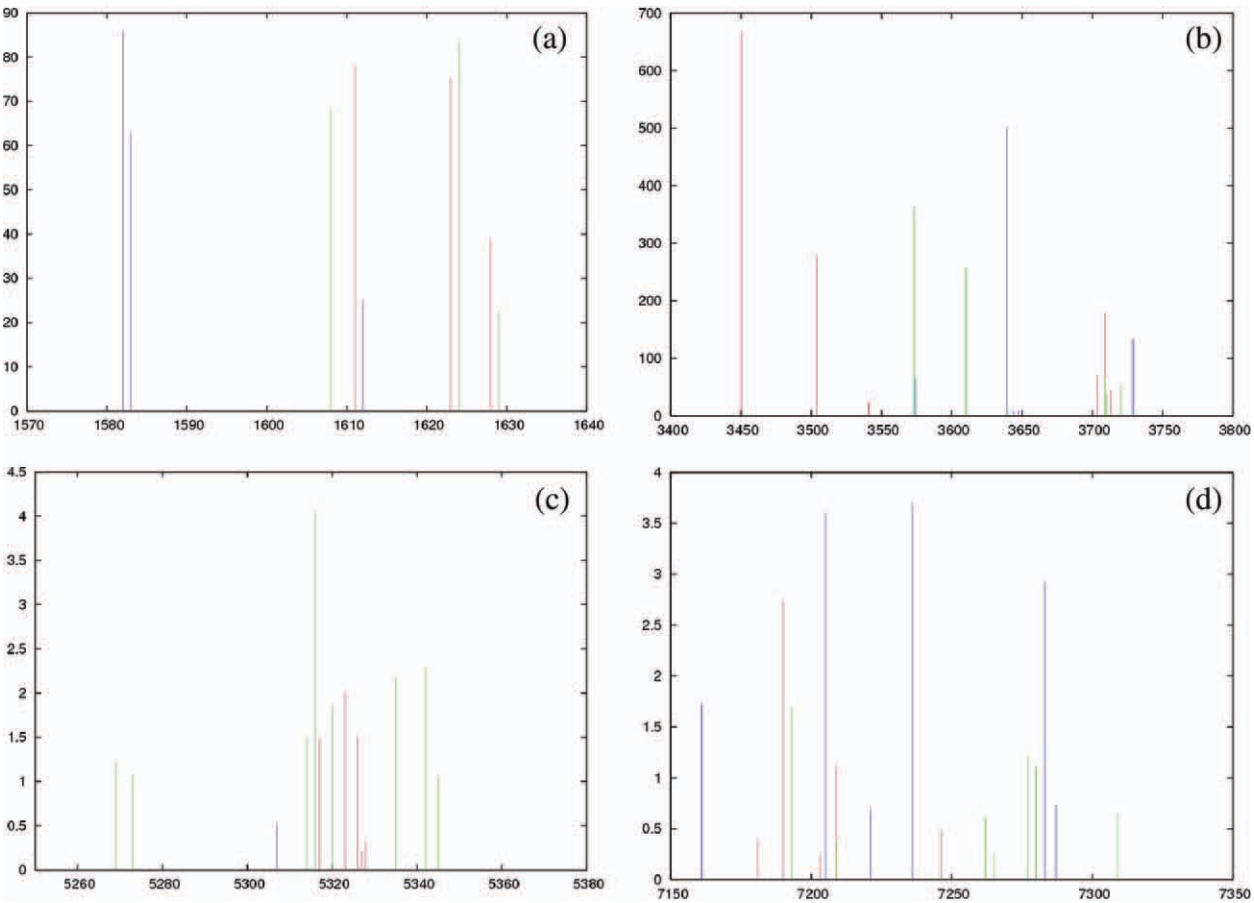

Figure 5. IR spectra of 4c (blue lines), 4d (green lines), and 4e (red lines) water trimers. Intensities are reported in km/mol. Quantum mechanical calcula tions including both mechanical and electrical anharmonicity determined at the B1LYP/cc pVTZ level. Four spectral regions were examined: a) HOH bend, ν_1 ν_3, [1570:1640] cm ^{1}, b) symmetrical and anti symmetrical OH stretching, ν_4 ν_9, [3400:3800] cm ^{1}, c) the first bend stretch combination band,[5250:5380] cm ^{1}, and d) the first stretch harmonic overtone ν_{OH}, [7150:7350] cm ^{1}.

i. The spectra of all four clusters cannot be mistaken one for another, particularly the OH stretching, depending on whether it is free or coupled into an H-bond. The differences for a given mode between the cyclic and linear forms is up to 200 cm^{-1};

ii. Intensities of corresponding modes are similar in each configuration.

iii. Modes of trimer 4d in the range [5250:5380] cm^{-1}, covering a broad spectral range, are up to twice as strong as those of the other clusters;

iv. Features in the spectral range [7150:7350] cm^{-1} are strongly coupled modes, hence difficult to assign. The main active modes in this region are combination modes ($\nu_6 + \nu_9$ 7193 cm^{-1}; 1.69 km/mol) and ($\nu_5 + \nu_8$ 7280 cm^{-1}; 1.12 km/mol), and the overtone of mode 8 corresponding to the asymmetrical OH stretch at 3883 cm^{-1} (7277 cm^{-1}; 1.21 km/mol). All trimer conformers share this behavior.[28]

v. Looking forward to a cluster-analysis of supercritical water,[27,44] note that the ν_{OH} modes in the range [7150:7350] cm^{-1} illustrate particularly well that neither the new cyclic trimer 4d nor the linear trimer 4c can explain the experimental data.[28] This discrepancy confirms the usefulness of step (3) of our strategy.

Inclusion of electrical anharmonicity is essential to such a study.

Conclusion and Outlook

The geometric structures of the clusters found with the present flexible TIP5P model compare well with the clusters deduced from quantum chemistry calculations (Table 4). Further quantum chemical minimization of the "classical" clusters leads to conformers found earlier in direct quantum chemistry optimizations,[27,28] lending confidence in use of the force field to perform molecular dynamics simulations of water in supercritical conditions. Analysis of these simulations should provide the water clusters prevalent at high temperatures and pressures. We now are working on a comparison of the clusters in supercritical water to the minimized structures identified so far.

A possible direction for improvement of the force-field is adjustment of the partial charges on L and H, dependent on neighborhood. The dipole moment of the flexible TIP5P model is about 2.3D to take into account the polarization effect of the neighborhood in liquid water under ambient conditions. In the clusters prevalent in supercritical water, the polarization effect is certainly much less, leading to an effective dipole much closer to the dipole of water in vacuum, around 1.84D. Another possibility is adjustment of the OL bond distance, inherited from TIP5P as 0.7 Å in the present 5-site flexible model. Because this distance reflects the size of the lone pair, it could be an adjustable parameter.

However, as we already know that even small differences between classical clusters and QM optimized structures can lead to significant spectral shifts and intensity discrepancies, it seems more fruitful to adhere to the strategy laid out in the introduction:

Preliminary screening by simulated annealing with a classical force-field, allowing very wide coverage of the potential energy surface, e.g., we here discovered a trimer missed in previous work;

Accurate QM minimization of the classical clusters followed by vibrational analysis to deduce its participation in the global IR spectrum.

Note that this coupled QM/MM approach is quite general and could be applied to other systems. Here, combining classical force-field screening with QM optimization provides a fast and accurate way to distinguish the relevant clusters involved in the IR spectrum of supercritical water. The method could be applied easily to other supercritical fluids, such as alcohol-water mixtures or other organic systems playing a key role in "green" chemistry.

Acknowledgments

We acknowledge the computational facilities provided by the computers of the MCIA-Mesocentre, University Bordeaux 1. We express our sincere gratitude to Pr Max Chaillet and to Pr Alain Dargelos for helpful discussions.

Keywords: quantum chemistry · molecular dynamics · water clusters · supercritical fluid

[1] M. C. Bellissent Funel, T. Tassaing, H. Zhao, D. Beysens, B. Guillot, Y. Guissani, *J. Chem. Phys.* **1997**, *107,* 2942.
[2] A. G. Kalinichev, S. V. Churakov, *Fluid Phase Equilib.* **2001**, *183 184,* 271.
[3] J. Marti, *Phys Rev* **2000**, *E61,* 449.
[4] L. B. Partay, P. Jedlovszky, I. Brovchenko, A. Oleinikova, *J. Phys. Chem. B* **2007**, *111,* 7603.
[5] D. Bo, F. S. Zhang, L. J. Zhao, *J. Hazard Mater.* **2009**, *170,* 66.
[6] P. E. Savage, *Chem. Rev.* **1999**, *99,* 603.
[7] T. Tassaing, Y. Danten, M. Besnard, *J. Mol. Liq.* **2002**, *101/1 3,* 149.
[8] Y. E. Gorbaty, A. G. Kalinichev, *J. Phys. Chem.* **1995**, *99,* 5336.
[9] K. Yamanaka, T. Yamaguchi, H. Wakita, *J. Chem. Phys.* **1994**, *101,* 9830.
[10] M. Bernabei, A. Botti, F. Bruni, M. A. Ricci, A. K. Soper, *Phys. Rev. E. Stat. Nonlin. Soft. Matter. Phys.* **2008**, *78,* 2.
[11] P. Wernet, D. Testemale, J. L. Hazemann, R. Argoud, P. Glatzel, L. G. M. Pettersson, A. Nilsson, U. Bergmann, *J. Chem. Phys.* **2005**, *123,* 154503.
[12] W. J. Lamb, G. A. Hoffman, J. Jonas, *J. Chem. Phys.* **1981**, *74,* 6875.
[13] M. M. Hoffmann, M. S. Conradi, *J. Am. Chem. Soc.* **1997**, *119,* 3811.
[14] N. Matubayasi, N. Nakao, M. Nakahara, *J. Chem. Phys.* **2001**, *114,* 4107.
[15] G. E. Walrafen, W. H. Yang, Y. C. Chu, *J. Phys. Chem. B* **1999**, *103,* 1332.
[16] D. M. Carey, G. M. Korenowski, *J. Chem. Phys.* **1998**, *108,* 2669.
[17] E. U. Franck, K. Roth, *Discuss Faraday Soc.* **1967**, *43,* 108.
[18] G. V. Bondarenko, Y. E. Gorbaty, *Mol. Phys.* **1991**, *74,* 639.
[19] Y. E. Gorbaty, G. V. Bondarenko, *Appl. Spectrosc.* **1999**, *53,* 908.
[20] Y. Jin, S. I. Ikawa, *J. Chem. Phys.* **2003**, *119,* 12432.
[21] A. Kandratsenka, D. Schwarzer, P. Vohringer, *J. Chem. Phys.* **2008**, *128,* 244510.
[22] D. Schwarzer, J. Lindner, P. Vohringer, *J. Phys. Chem. A* **2006**, *110,* 2858.

[23] T. I. Mizan, P. E. Savage, R. M. Ziff, In Innovations in Supercritical Fluids: Science and Technology, Vol. *608; K. W. Hutchenson, N. R. Foster, Eds.; ACS: Washington D.C.,* **1995**; p. 47.
[24] K. M. Benjamin, A. J. Schultz, D. A. Kofke, *J. Phys. Chem. B* **2009**, *113,* 7810.
[25] M. Boero, K. Terakura, T. Ikeshoji, C. C. Liew, M. Parrinello, *J. Chem. Phys.* **2001**, *115,* 2219.
[26] A. G. Kalinichev, S. V. Churakov, *Chem. Phys. Lett.* **1999**, *302,* 411.
[27] D. Bégué, I. Baraille, P. A. Garrain, A. Dargelos, T. Tassaing, *J. Chem. Phys.* **2010**, *133,* 034102.
[28] T. Tassaing, P. A. Garrain, D. Bégué, I. Baraille, *J. Chem. Phys.* **2010**, *133,* 034103.
[29] W. Smith, *Mol. Simul.* **2006**, *32,* 933.
[30] P. A. Cazade, P. Bordat, I. Baraille, R. Brown, W. Smith, I. T. Todorov, *Mol. Simul.* **2011**, *37,* 43.
[31] G. Strey, *J. Mol. Spectrosc.* **1967**, *24,* 87.
[32] G. Rauhut, G. Knizia, H. J. Werner, *J. Chem. Phys.* **2009**, *130,* 054105.
[33] N. Gohaud, D. Bégué, C. Pouchan, *Chem. Phys.* **2005**, *310,* 85.
[34] N. Gohaud, D. Bégué, C. Pouchan, *Int. J. Quantum Chem.* **2005**, *104,* 773.
[35] D. Bégué, N. Gohaud, C. Pouchan, P. Cassam Chenaï, J. Lievin, *J. Chem. Phys.* **2007**, *127,* 164115.
[36] L. A. Curtis, D. L. Frurip, M. J. Blander, *J. Chem. Phys.* **1979**, *71,* 2703.
[37] D. A. Estrin, L. Paglieri, G. Corongiu, E. Clementi, *J. Phys. Chem.* **1996**, *100,* 8701.
[38] A. G. Kalinichev, Y. E. Gorbaty, A. V. Okhulkov, *J. Mol. Liq.* **1999**, *82,* 57.
[39] G. S. Fanourgakis, X. Xantheas, *J. Chem. Phys.* **2008**, *128,* 074506.
[40] X. Huang, B. J. Braams, J. M. Bowman, R. E. A. Kelly, J. Tennyson, G. C. Groenenboom, A. van der Avoird, *J. Chem. Phys.* **2008**, *128,* 034312.
[41] W. S. Benedict, N. Gaillan, E. K. Plyer, *J. Phys. Chem.* **1956**, *24,* 1139.
[42] A. F. A. Vilela, P. R. P. Barreto, R. Gargano, C. R. M. Cunha, *Chem. Phys. Lett.* **2006**, *427,* 29.
[43] K. Kuchitsu, Y. Morino, *Bull. Chem. Soc. Jpn.* **1965**, *38,* 805.
[44] M. Y. Tretyako, D. S. Makaro, *J. Chem. Phys.* **2011**, *134,* 084306.